International Journal of Design & Nature and Ecodynamics
Vol. 21, No. 2, February, 2026, pp. 299-316
Journal homepage: http://iieta.org/journals/ijdne

Impacts of Land Use/Land Cover Changes on Water Quality in the Upper Brantas Watershed: A Spatio-Temporal Analysis Using Riparian Buffer Approach

Lintang Suska Hariwati[1,2*], Anthon Efani[3], Fitri Candra Wardana[1], Muhammad Fathur Rouf Hasan[1]

[1] Department of Environmental Resources Management and Development, Universitas Brawijaya, Malang 65145, Indonesia
[2] East Java Provincial Environmental Agency, Surabaya 60234, Indonesia
[3] Faculty of Fisheries and Marine Science, Universitas Brawijaya, Malang 65145, Indonesia

Corresponding Author Email: anthonefani@ub.ac.id

https://doi.org/10.18280/ijdne.210201

Received: 26 November 2025
Revised: 14 January 2026
Accepted: 22 January 2026
Available online: 28 February 2026

Keywords:
LULC dynamics, Euclidean distance buffer, surface water quality, Sentinel-2 imagery, spatial-temporal analysis, principal component analysis, Brantas River Basin

ABSTRACT

The Brantas River Basin accounts for roughly 25% of East Java's watershed area and is facing increasing environmental pressure driven by land use and land cover (LULC) changes, particularly in the upstream region. Alterations within riparian zones can strongly influence surface water quality, yet spatio-temporal assessments using Euclidean distance–based approaches remain limited. This study examines the relationship between LULC dynamics and surface water quality in the upstream Brantas Basin from 2020 to 2025. Water quality data were collected from three monitoring stations during wet and dry seasons, covering eight physical, chemical, and biological parameters. LULC classification was generated from ESRI Sentinel-2 imagery and processed using Geographic Information Systems. Descriptive statistics, correlation analysis, and principal component analysis (PCA) were applied to assess spatial–temporal patterns and identify parameters most sensitive to land-use changes. Results show that the upstream sub-watershed consists of four dominant LULC classes: built-up areas, croplands, forested areas with vegetation > 15 m, and water bodies. Between 2020 and 2025, built-up areas and croplands expanded by 3.4% and 3.2%, while forested areas declined by 7.4%. Despite several parameters meeting regulatory thresholds, water quality degradation was indicated by increasing concentrations of chemical oxygen demand (COD), total suspended solids (TSS), and fecal coliform. Spearman correlation analysis reveals that built-up riparian areas are the dominant LULC factor influencing water quality, exhibiting strong to very strong correlations with TSS ($\rho = -0.131$ to 0.953) and COD ($\rho = -0.393$ to 0.926) across monitoring stations. These results show that stricter riparian protection and land-use control are needed, especially in growing cities, to effectively reduce sediment and organic pollution in the upstream Brantas Basin.

1. INTRODUCTION

Land conversion from natural habitats into built-up landscapes continues to escalate and has become one of the primary drivers of ecological degradation, particularly through the emergence of non-point source pollution transported by diffuse runoff into river systems [1]. Within watershed environments, anthropogenic pressures—including urban expansion, agricultural intensification, and vegetation loss—have been widely recognized as major contributors to river water quality decline, evidenced by elevated pollutant loads such as sediments, nutrients, and organic contaminants [2, 3]. These impacts are further complicated by the spatial and temporal variability of landscape characteristics such as topography, soil properties, hydrology, and climate, which shape the complex relationship between land use and land cover (LULC) patterns and surface water quality [4]. In East Java Province, spatial–temporal trends from 2015 to 2024 indicate substantial shifts in LULC, including considerable increases in settlement areas and dryland agriculture, alongside marked reductions in forest cover [5]. These trends parallel the declining performance of key environmental indicators, particularly the water quality index (WQI) and land quality index (LQI), both of which form essential components of the national environmental quality index (IKLH). Data from the Ministry of Environment and Forestry (KLHK) reveal a long-term downward trend in WQI and LQI across East Java from 2015 to 2024, signaling growing ecological stress associated with riparian degradation and intensifying land-use pressures [6].

LULC degradation in East Java has been persistent over the last fifty years, significantly impacting regional hydrological dynamics, particularly in the Brantas watershed, which is most ecologically sensitive in its upper reaches [7, 8]. Previous studies indicate that alterations in land use along the Upper Brantas River correlate with a deterioration in water quality and the river ecosystem's health, as evidenced by physicochemical parameters and biological indicators, including macrozoobenthos [9, 10].

Recent assessments of the Brantas River further

demonstrate that several river segments fall within the "poor" water quality category and no longer meet the designated Class II standards, with water quality showing progressive deterioration over time due to forest degradation, urbanization, and industrial expansion in the upper watershed [11, 12]. These findings indicate that water quality degradation induced by LULC change represents a consistent ecological pattern across tropical watersheds in East Java [13]. Considering the essential ecological role of riparian zones—serving as biophysical filters that reduce sediment, nutrients, and contaminants [14]—spatial analysis focusing on riparian buffer areas has become increasingly relevant for understanding how LULC dynamics influence water quality across different spatial scales. Employing Euclidean-distance–based riparian buffers enables more precise identification of critical areas that disproportionately affect river water conditions.

Previous studies in several Indonesian watersheds have consistently revealed strong correlations between LULC patterns and water quality parameters, such as in the Ciliwung River, Bekasi River, and Jeneberang watershed [15-17]. At a smaller spatial scale, urban land cover has been identified as one of the most influential drivers of water quality degradation [18]. However, quantitative approaches that explicitly link spatio-temporal LULC dynamics within riparian buffer zones to variations in water quality parameters through regression-based models remain limited in the Upper Brantas River, despite the recognized role of riparian areas as primary natural filters of runoff and pollutant loads. Therefore, this study offers a novel methodology by integrating multi-scale Euclidean-based riparian buffer analysis with spatio-temporal regression modeling to quantify the relative contribution of LULC transitions to surface water quality degradation in a specific Upper Brantas sub-watershed. This approach provides a more precise, evidence-based foundation for identifying critical riparian zones, formulating targeted protection strategies, and improving environmental management performance in East Java. The scope of this research is limited to river surface water quality, three monitoring stations, Sentinel-2 imagery with 10 m spatial resolution, and riparian vegetation analysis within 500 m and 1000 m Euclidean distances from sampling points.

2. METHODS

2.1 Study area

This study was conducted in the Upper Brantas watershed (238,148 ha), East Java, Indonesia, which covers Batu City, Malang City, Malang Regency, and Blitar Regency and constitutes one of the most ecologically sensitive headwater river systems in the region. Rather than being treated as separate geomorphological units, the Ambang, Lesti, and Melamon sub-watersheds form an integrated upstream river network draining a landscape that has undergone a progressive transition in LULC from natural forest to urban settlements and intensive agriculture. In this context, the present study does not emphasize river length or sub-basin size, as its primary objective is to evaluate how spatial LULC gradients regulate river water quality. The conversion of large areas of forest into agricultural land and residential areas since 2009 has been documented in previous studies. Widespread land use incompatibility, where agricultural activities have encroached on protected zones, has resulted in increased surface runoff, erosion, and pollutant mobilization [19-23].

Three water quality monitoring stations were strategically selected along the Upper Brantas River, namely ST1 (Arboretum Sumber Brantas) in Batu City, ST2 (Gadang Bridge) in Malang City, and ST3 (Kalipare Bridge) in Malang Regency. The purpose of this is to explicitly capture the LULC gradient. ST1 represents the upstream zone, which is dominated by forests, characterized by high vegetation cover, volcanic soil, and little anthropogenic disturbance. It plays a critical role in regulating hydrological processes and maintaining basic water quality [24]. ST2 is an urban transition zone characterized by mixed land use, rapid urban expansion, road infrastructure, and increased impervious surface cover and residential-commercial development that has altered natural water flow paths, resulting in increased pollutant loads, sediment input, and greater hydrological variability [9, 24]. ST3 is located downstream in the upper watershed. This zone is primarily affected by intensive agricultural activities, including irrigated agricultural land and hillside horticulture, where extensive conversion of forest and mixed vegetation has significantly affected soil stability, nutrient flow, and river water quality [24, 25]. The sequential arrangement of ST1–ST3 (Table 1), therefore, represents a typical and well-defined LULC gradient, from forest to urban to agricultural landscapes, providing a robust spatial framework for evaluating how progressive land-use transitions control hydrological processes and water-quality dynamics in the Upper Brantas watershed.

Table 1. Brantas River monitoring location points

No.	Location	LS	BT	Description
1	Arboretum Brantas (ST1)	-7.759306	112.528056	The upper reaches of the Brantas River, located in the Arboretum, a location that is expected to be free of pollution
2	Jembatan Gadang (ST2)	-8.02444	112.63289	Urban Areas
3	Jembatan Kalipare (ST3)	-8.1565556	112.4343333	Semi-urban, with most of the area being dryland agriculture

Note: LS denotes South Latitude (Lintang Selatan), and BT denotes East Longitude (Bujur Timur).

This gradient-based design underpins the spatio-temporal riparian buffer analysis used in this study to identify landscape units that most strongly contribute to water-quality degradation. The locations of all monitoring stations in the upper reaches of the Brantas River can be seen in Figure 1.

2.2 Water quality data

Thirty-six surface water samples were collected between 2020 and 2025. The data represents the rainy and dry seasons with a frequency of twice a year. Water quality data for the 2021–2024 period and the 2025 rainy season were obtained from the East Java Provincial Environment Agency. Meanwhile, data for the 2025 dry season were taken from field

sampling on August 6–7, 2025. To ensure hydrological suitability, all sampling was carried out under stable base flow conditions, excluding periods with rainfall exceeding 10 mm in the previous 24 hours. River water was collected using a cross-sectional composite sampling approach. At ST3 (±35 m wide), samples were taken at three points (left bank, mid-channel, and right bank); at ST2 (< 20 m wide), at two points (1/3 and 2/3 of the channel width); and at ST1 (< 10 m wide), at a single mid-channel point. River widths were estimated from high-resolution satellite imagery (Google Earth). Sub-samples were combined to obtain a composite sample representing the mean physicochemical and microbiological condition of each river cross-section. Although flow velocity was not measured directly, restricting sampling to baseflow conditions minimized discharge-driven variability.

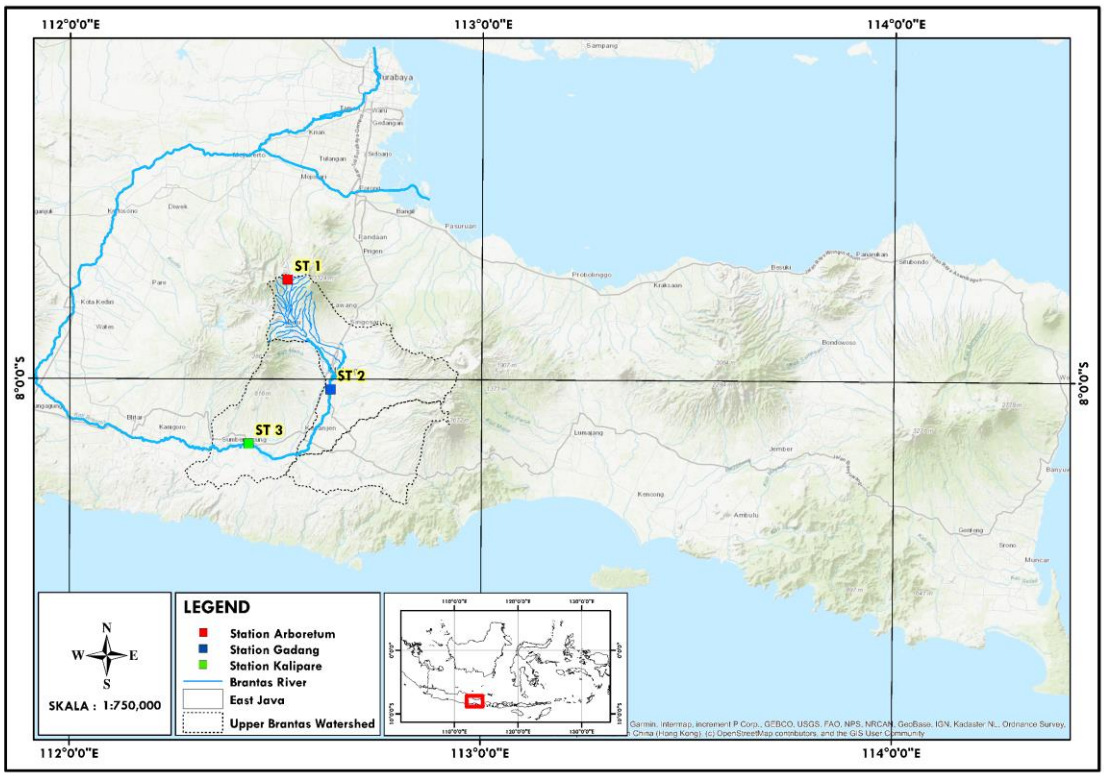

(a)

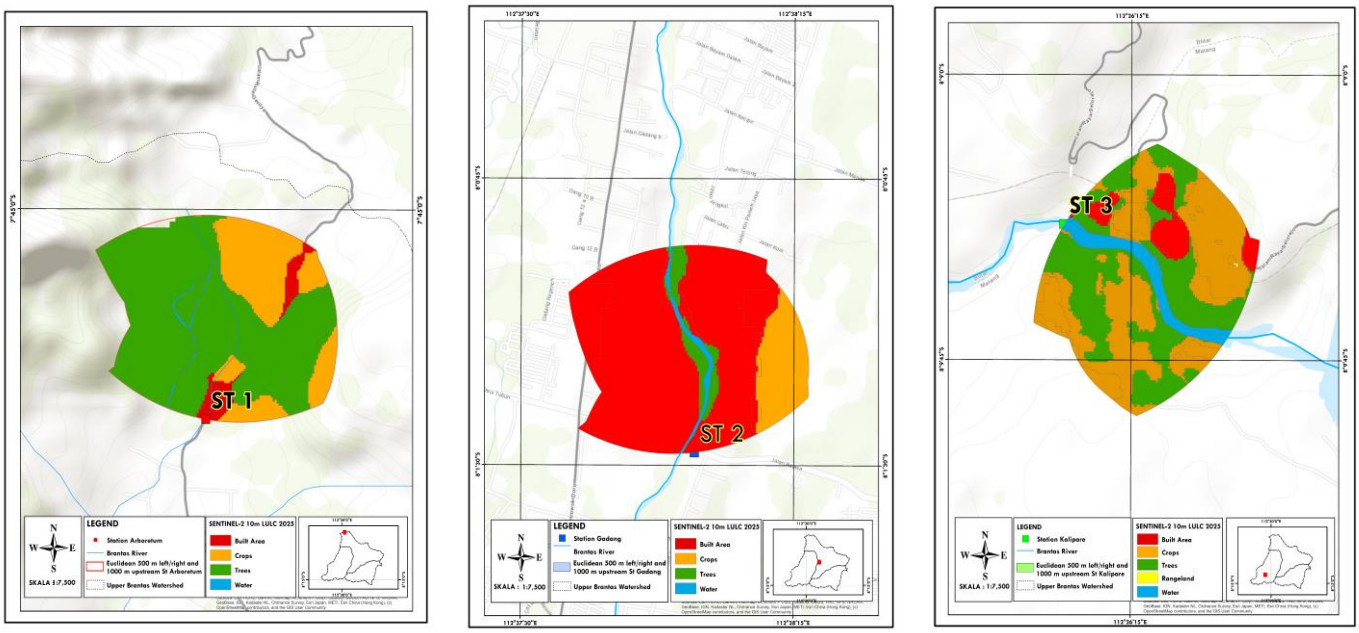

(b)

Figure 1. (a) Sampling locations and land use/land cover (LULC), red, blue, and green panels refer to the ST. Arboretum, ST Gadang, ST Kalipare Monitoring Station, and (b) Euclidean scale riparian zone 500m left/right of the river boundary and 1000 m upstream of the monitoring station

Table 2. Summary of water quality in the Upper Brantas sub-watershed from three monitoring stations for the 2020-2025 period

Parameter Unit	pH mg/L	BOD mg/L	COD mg/L	TSS mg/L	DO mg/L	NO_3 mg/L	TP mg/L	FC mg/L
Mean	7.55	2.59	11.84	24.53	6.20	2.07	0.16	11,265.58
Dev	0.27	1.31	7.11	43.05	2.12	1.19	0.11	30,094.07
Median	7.58	2.43	10.65	4.70	6.57	2.11	0.10	104.50
Min	6.41	0.48	2.90	-	2.00	0.41	0.04	-
Max	8.00	5.92	32.00	167.00	9.00	4.50	0.43	111,990
Standard Error	0.05	0.22	1.20	7.28	0.36	0.20	0.02	5,086.83
Kurtosis	7.02	0.60	1.12	4.76	-1.05	-0.81	0.28	6.72
Skewness	-1.97	0.90	1.04	2.34	-0.39	0.12	1.26	2.82
Quality Standard Class I	6-9	2	10	40	6	10	0.2	100
Quality Standard Class II	6-9	3	25	50	4	10	0.2	1000

Eight parameters were analyzed: total suspended solids (TSS), dissolved oxygen (DO), pH, biochemical oxygen demand (BOD), chemical oxygen demand (COD), NO_3-N, total phosphorus (T-P), and fecal coliform, following Appendix VI of Government Regulation No. 22 of 2021 [26]. DO and pH were measured but not treated as latent variables in the LULC–water quality analysis because they primarily act as response indicators. Water quality was evaluated against the Class II standard, which corresponds to water supply, fisheries, recreation, and ecosystem protection functions and provides a conservative and environmentally relevant benchmark for the Upper Brantas River. Mean values for 2021–2025 were computed and compared with Class II thresholds. Relationships between LULC composition within riparian buffers and water quality parameters were assessed using correlation and regression analyses to identify dominant land-use drivers of water quality degradation along the Upper Brantas River. Table 2 provides a summary of the water quality monitoring data from 2020 to 2025.

2.3 Spatial datasets acquisition and pre-processing

Primary and secondary data were collected for LULC change analysis. Field observations and exploratory surveys were conducted to better understand the dominant land use patterns around the Arboretum Sumber Brantas station. Sentinel-2 LULC data for 2021–2024 were obtained from the ESRI Living Atlas Global Land Cover dataset, which provides 10-m resolution annual land-cover maps derived from Sentinel-2 imagery. Although CNN-based semantic segmentation (e.g., U-Net) is widely used for Sentinel-2 land-cover mapping, this study employed the ESRI Living Atlas Global Land Cover product for 2021–2024, which is generated using a globally trained CNN (U-Net–type) deep-learning model applied to Sentinel-2 imagery. Because the classification was produced using ESRI's pretrained model, no site-specific CNN training samples were required in this study, and the ESRI LULC maps were used as analysis-ready deep-learning outputs for subsequent spatio-temporal analysis in the Upper Brantas Basin. This product represents analysis-ready data, in which atmospheric correction, cloud masking, mosaicking, and temporal compositing have already been applied by ESRI prior to classification.

Sentinel-2 images for 2025 (January–August, 2025) were acquired from the Copernicus Open Access Hub and processed using QA60-based cloud and cirrus masking, followed by median compositing to ensure temporal and spatial consistency across years. The 2025 composite was classified using the same ESRI-based LULC legend and decision rules to ensure consistency with the pretrained CNN-derived maps for 2021–2024. All spectral bands were resampled to 10 m and stacked using visible, near-infrared, and short-wave infrared bands for classification. Eight LULC classes were defined based on vegetation structure and land-use characteristics: dense forest (> 15 m), mixed tree vegetation (5–15 m), shrubs/grasslands (< 5 m), cropland, built-up surfaces, bare land, water bodies, and wetlands, representing the dominant forest–urban–agriculture gradient across the Upper Brantas Basin (ST1–ST3) [27]. Raster data on LULC from 2021 to 2025 (Table 3) were further processed and analyzed using ArcGIS Pro to assess variations in land cover over time.

Table 3. Description of spatial datasets used in this study

Satellite Data	Acquisition Date (Composite Images)	Spatial Resolution
Sentinel – 2 (land use/ land cover) ESRI	3 January-31 August 2025	10 meter
	3 January-31 December 2024	10 meter
	4 January-31 December 2023	10 meter
	4 January-31 December 2022	10 meter
	4 January-31 December 2021	10 meter

Accuracy in this study was assessed using the overall accuracy (OA) and Kappa coefficient (κ) metrics. These metrics provide additional insight into the reliability of classified maps. The calculations follow a methodology that has been tested in spatial analysis. OA is one of the simplest and most intuitive accuracy metrics. The metric is calculated as the proportion of pixels (or units) that are classified correctly in the dataset relative to the total number of pixels in the classification results. The Kappa coefficient (κ), meanwhile, is a more robust measure of classification accuracy. Kappa measures the degree of agreement between the classification results and the reference data while taking into account the possibility of random agreement. In this study, these accuracy metrics were derived from an independent set of homogeneous reference units for local validation of the ESRI LULC product, rather than from a probability-based pixel sampling design intended to estimate basin-wide map accuracy. The Kappa coefficient penalizes agreements that occur by chance, making it useful for handling unbalanced datasets. The following formula is used for OA.

$$OA = \frac{Total\ of\ Correctly\ Classified\ Pixels}{Total\ Number\ of\ Reference\ Pixels} \quad (1)$$

OA provides a straightforward assessment of the proportion of correct classifications, but it has limitations. Particularly, it does not account for the possibility of random agreement between the classification result and the reference data [28]. The Kappa coefficient is calculated using the following formula:

$$\kappa = \frac{P_o - P_e}{1 - P_e} \quad (2)$$

In this context, P_o represents the proportion of cases that are correctly classified, which is essentially the OA of the classification. On the other hand, P_e refers to the expected proportion of cases that would be correctly classified purely by chance. It's important to note that in this notation, the difference between parameters and estimated parameters isn't explicitly stated, but the text will clarify where estimates based on samples are being applied or utilized [29]. A Kappa value greater than 0.60 is typically considered an acceptable level of agreement. Kappa is generally interpreted as the result $0.81 \leq \kappa \leq 1.00$, considered as almost perfect agreement.

2.4 Principal component analysis

Principal component analysis (PCA) was used to determine the main water parameters in the dataset variation [15]. The varimax rotation technique was used to explain the most significant water quality parameters affecting the variability in the water quality data. The validity of the PCA results was evaluated using the Kaiser-Meyer-Olkin (KMO) test and Bartlett's sphericity test. High values close to 1 on the KMO test and values less than 0.05 on the Bartlett test indicate that PCA is increasingly useful for application to water quality data [30].

2.5 Statistical analysis

Descriptive statistics were employed to ascertain the mean, standard deviation (SD), median, standard error (SE), skewness, kurtosis, and the minimum and maximum ranges of water quality in the Upper Brantas sub-basin across various seasons. The assessment of the impact of LULC on water quality involved computing the correlation between the measured water quality variables and the percentage of LULC areas [15, 31]. Correlation analyses were conducted utilizing IBM SPSS Statistics version 25 software to verify the linear relationship between the dependent variables of water quality (TSS, BOD, COD, NO_3-N, T-P, and fecal coli) and the independent variables of LULC [3]. Correlation coefficients elucidate the nature of the relationship between two variables, indicating whether it is positive, negative, or absent.

3. RESULTS

3.1 Spatio-trend of Upper Brantas watershed quality

The lowest temperatures were observed at ST1 in both seasons, with median values ranging from 17-18 °C in the rainy season and dry season. ST2 and ST3, by contrast, showed higher temperatures, with median values of around 26-28 °C in the rainy season and 25-29 °C in the dry season. The temperature distribution at ST1 was relatively narrow in both seasons, while ST2 and ST3 showed a wider interquartile range, especially in the rainy season. This spatial-temporal pattern is consistent throughout the seasons, with the sequence ST1 < ST2 ≈ ST3. The highest DO values were observed at ST1 (around 8-9 mg/L) in both seasons, followed by ST2 (around 6-7 mg/L in the rainy season and 5-6 mg/L in the dry season). The lowest median value was observed in ST3 (around 3-4 mg/L). The highest and most variable TSS value was observed at ST2, with values above 150 mg/L during the rainy season and decreasing to around 20–50 mg/L during the dry season.

Meanwhile, ST1 and ST3 remained below 20 mg/L in both seasons. BOD and COD followed comparable spatial patterns. The median BOD value was around 2 mg/L in ST1, 3–4 mg/L in ST3, and 4–5 mg/L in ST2, while the median COD value was around 6–8 mg/L in ST1 and 15–25 mg/L in ST2 and ST3. Nitrate (NO_3^-) concentrations were lowest at ST1 (generally < 2 mg/L), moderate at ST3 (approximately 2–3 mg/L), and highest at ST2 (approximately 3–5 mg/L). The median total phosphate (TP) ranged from approximately 0.1–0.2 mg/L in ST1 and ST3 to 0.3–0.4 mg/L in ST2. The fecal coliform count was much higher in ST2, with values exceeding 10^3 MPN 100 mL^{-1} in both seasons, while ST1 and ST3 remained close to the lower measurement range. At all stations, pH remained within a narrow neutral range (approximately 7.2–7.8) in both seasons. Compared to the Class II criteria of PP 22/2021, the distribution of DO, organic, nutrient, and microbiological parameters placed ST1 closer to the Class II range, while ST2 and ST3 showed higher values and wider variability for several parameters. Figure 2 shows the spatial and seasonal distributions of water temperature, TSS, BOD, and COD across ST1–ST3.

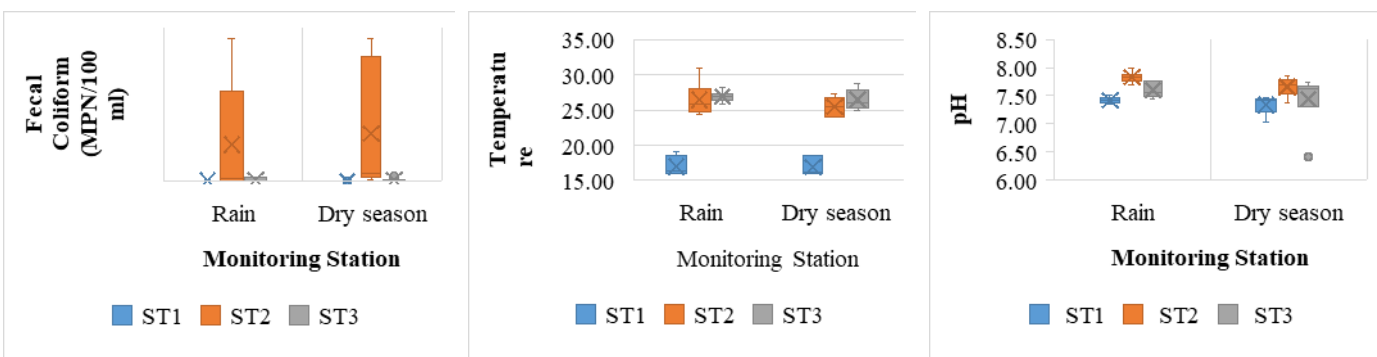

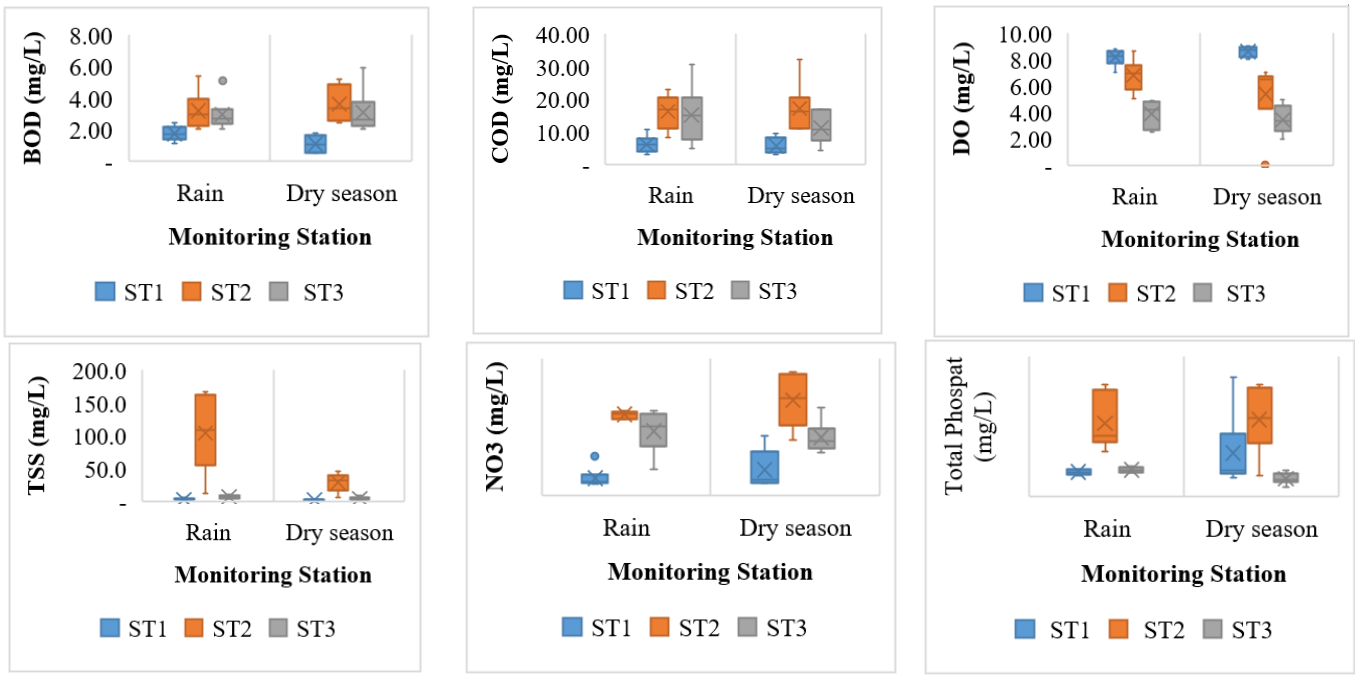

Figure 2. Spatio-trend of Upper Brantas watershed quality

3.2 Temporal trend of Upper Brantas watershed quality

Box plots for water quality parameters from 2020 to 2025 are presented in Figures 3 and 4. BOD values were high and had a wide interquartile range from 2020 to 2021. These values decreased and became more stable from 2022 to 2025. BOD values ranged from 2.0 to 2.5 mg/L. From 2020 to 2023, DO and pH were measured within a relatively small range. pH values remained close to neutral to slightly alkaline (around 7.0 to 8.0). In 2025, the range of DO and pH values is smaller than in previous years.

The median COD value increases, and the interquartile range widens from 2021 to 2024. The highest values are recorded in 2023–2024, then decrease slightly in 2025. There was significant variation in TSS from year to year, with high median values and wide dispersion in 2021, 2023, and 2025. There are several outlier values where the concentration exceeds 100 mg/L. Starting in 2022, the median values of NO_3^- and TP began to increase. The highest fecal coliform concentrations were consistently recorded at station ST2. The time series graph shows that BOD values were higher in 2020–2021 and again in 2025 compared to the intervening years. DO showed lower values during the dry season observations at ST2 compared to other stations. During the period 2020–2025, all parameters showed clear temporal and spatial variability, as reflected in changes in the median, interquartile range, and outlier values in the annual distribution.

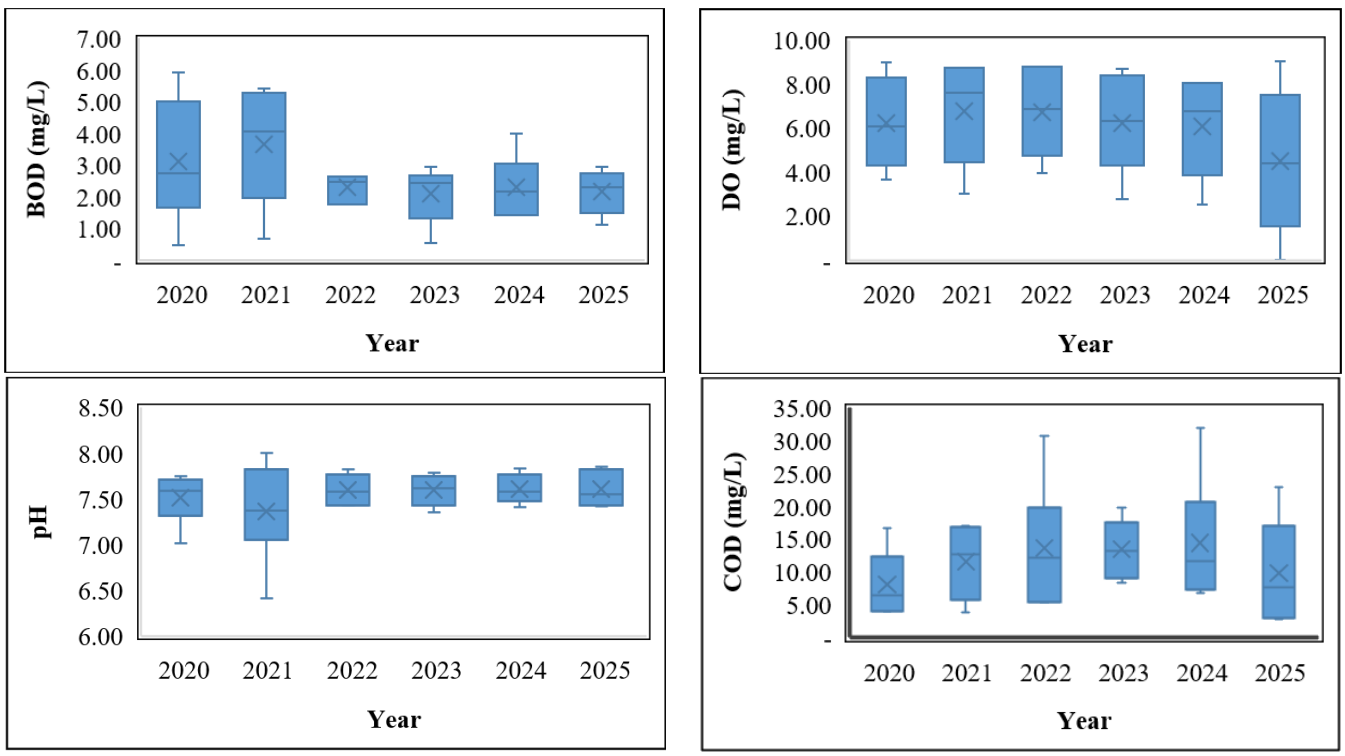

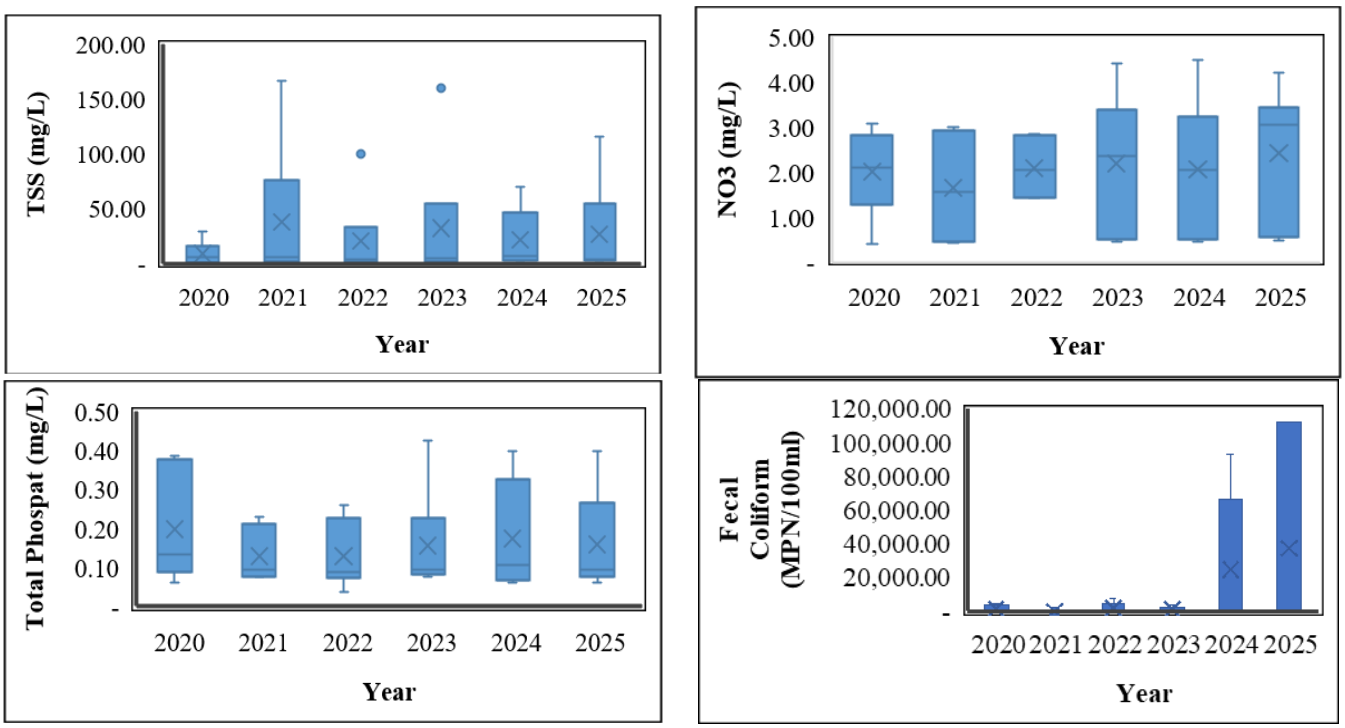

Figure 3. Temporal trend of Upper Brantas watershed quality

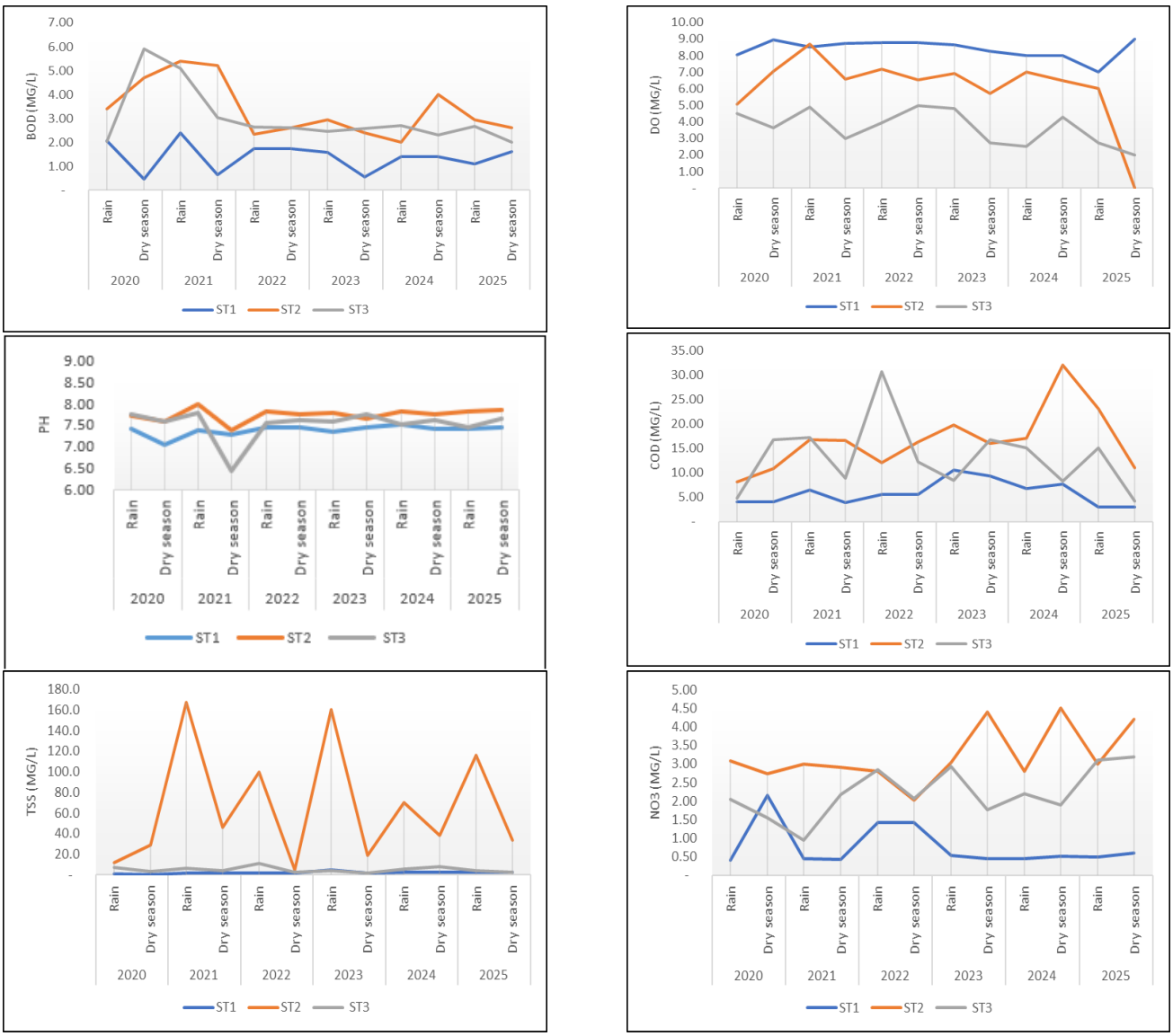

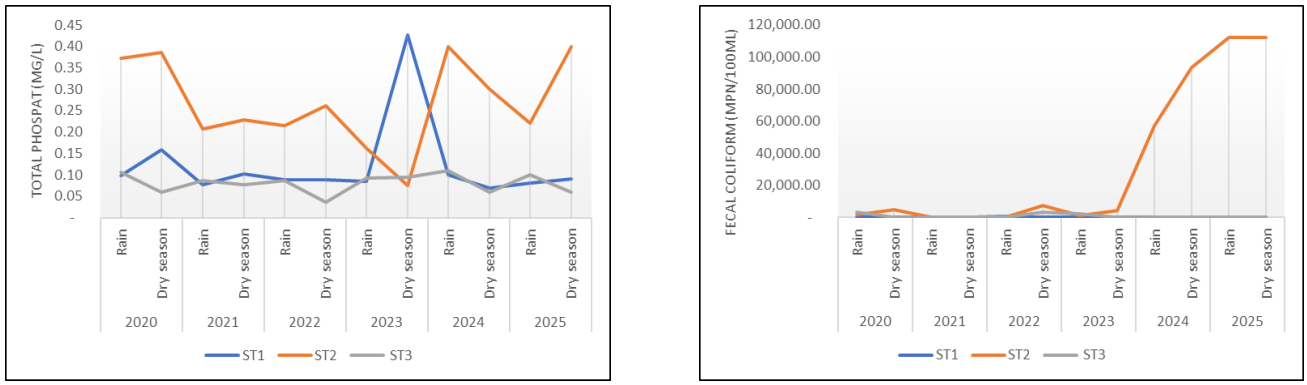

Figure 4. Time series of water quality parameters of the Upper Brantas watershed

3.3 LULC, changes, and urbanization rates in the Upper Brantas sub-watershed

Eight land-cover classes were mapped from Sentinel-2 imagery for the period 2020–2025 using the ESRI Living Atlas Global Land Cover product. The classes comprise built-up area, rangeland, trees, bare ground, crops, flooded vegetation, and water. The spatial distribution and areal proportions of these classes for the Upper Brantas sub-basin are summarized in Table 4.

The 2025 imagery in this study was not retrained using the CNN-UNet model; its performance was evaluated in the Brantas upstream sub-region using an independent local reference dataset. Based on 100 spatially homogeneous reference units, the confusion matrix (Table 5) yielded a local OA of 91% and a Kappa coefficient (κ) of 0.873. Users' and Producer's accuracies for each class are reported in Table 5. These statistics represent a site-specific consistency check of the ESRI CNN-UNet LULC product and are not intended to replace or replicate the global validation reported by ESRI.

Table 4. The LULC classification in the Upper Brantas sub-basin

LULC Classification	2020		2021		2022		2023		2024		2025		% LULC Change 2020-2025
	Area (Ha)	%	Area (Ha)	%	Area (Ha)	%	Area (Ha)	%	Area (Ha)	%	Area (Ha)	%	
Air (Water)	2,011.56	0.8%	1,991.08	0.8%	2,024.66	0.8%	1,939.22	0.8%	1,939.22	0.8%	1,877.40	0.8%	-0.1%
Area Terbangun (Build Area)	65,077.39	26.1%	66,235.19	26.6 %	71,328.46	28.7%	73,563.24	29.6%	73,563.24	29.6%	73,518.99	29.6%	3.4%
Awan (Clouds)	85.10	0.0%	104.70	0.0%	2.80	0.0%	91.44	0.0%	91.44	0.0%	92.84	0.0%	0.003%
Padang Rumput (Rangeland)	3,578.18	1.4%	2,472.95	1.0%	5,937.42	2.4%	5,641.26	2.3%	5,641.26	2.3%	5,651.17	2.3%	0.8%
Pohon (Trees)	104,406.83	41.9%	104,616.16	42.0 %	84,461.45	33.9%	85,910.05	34.5%	85,910.05	34.5%	85,813.72	34.5%	-7.4%
Tanah Terbuka (Bare Gound)	13.68	0.01%	13.80	0.01 %	13.62	0.01%	19.36	0.01%	19.36	0.01%	19.60	0.01%	0.002%
Tanaman (Crops)	73,743.74	29.6%	73,482.32	29.5 %	85,149.06	34.2%	81,751.62	32.8%	81,751.62	32.8%	81,570.43	32.8%	3.2%
Vegetasi Tergenang (Flooded Vegetation)	3.87	0.002 %	4.15	0.002 %	2.88	0.001%	4.16	0.002%	4.16	0.002%	4.17	0.002%	0.0001%
	248,920.35	100	248,920.35	100	248,920.35	100	248,920.35	100	248,920.35	100	248,920.35	100	

Table 5. Confusion matrix–based local validation of the ESRI CNN-UNet LULC product (2025) for the Upper Brantas Basin

LULC Class	Water	Trees	Flooded Vegetation	Crops	Built Area	Bare Ground	Rangeland	Total	User's Accuracy (UA, %)	Local OA (%)	Local κ
Water	15	0	0	0	0	0	0	15	100.00%	0	0
Trees	0	28	0	4	0	0	0	32	87.50%	0	0
Flooded Vegetation	0	0	1	0	0	0	0	1	100.00%	0	0
Crops	0	0	0	21	1	0	0	22	95.45%	0	0
Built Area	0	2	0	3	21	0	0	26	80.77%	0	0
Bare Ground	0	0	0	0	0	3	0	3	100.00%	0	0
Rangeland	0	0	0	0	0	0	1	1	100.00%	0	0
Column Total	15	30	1	28	22	3	1	100	100.00%	0	0
PA (%)	100.00%	93.33%	100.00%	75.00%	95.45%	100.00%	100.00%	100.00%	0	0	0

Local OA = 91.0%, Local κ = 0.873.

UA = user's accuracy; PA = producer's accuracy; OA = overall accuracy; κ = Kappa coefficient. This confusion matrix is based on 100 spatially homogeneous reference units and provides a site-specific validation of the ESRI CNN-UNet LULC product for 2025. The resulting Local OA and Local κ represent a local consistency check within the Upper Brantas sub-basin and should not be interpreted as statistically representative accuracy estimates for the entire watershed or as a replication of the global ESRI validation.

Table 5 summarizes the local agreement between the ESRI LULC classification and independent reference data for 2025, highlighting class-specific commission and omission patterns within the study area. Analysis of land cover changes between 2020 and 2024 shows a decrease in cover class, namely a 7.4% decrease in the percentage of tree area (trees) and a 0.028% decrease in water area (water). However, on the other hand, there was an increase in the area of built-up area (built-up area) by 3.4% and crops (crops) by 3.2% in the Upper Brantas sub-basin. A significant decrease in the percentage of tree area occurred in the 2021-2022 period, where the 42.2% tree cover area in 2021 decreased to 34.1% of the total area of the Brantas sub-basin. The distribution of land cover classes is presented in Figure 5.

3.4 Land use/land cover, and habitat quality at the Euclidean scale

The LULC composition within a 1000-meter Euclidean riparian zone upstream and 500 meters to the right/left of the river boundary at three Monitoring Stations is shown in Figure 6. The area of each land cover class was obtained from the Euclidean distance, which was then expressed as a percentage of the total area. Figure 7 shows the temporal evolution of built-up, cropland, and forest proportions within the riparian buffer zones of ST1, ST2, and ST3 between 2020 and 2025.

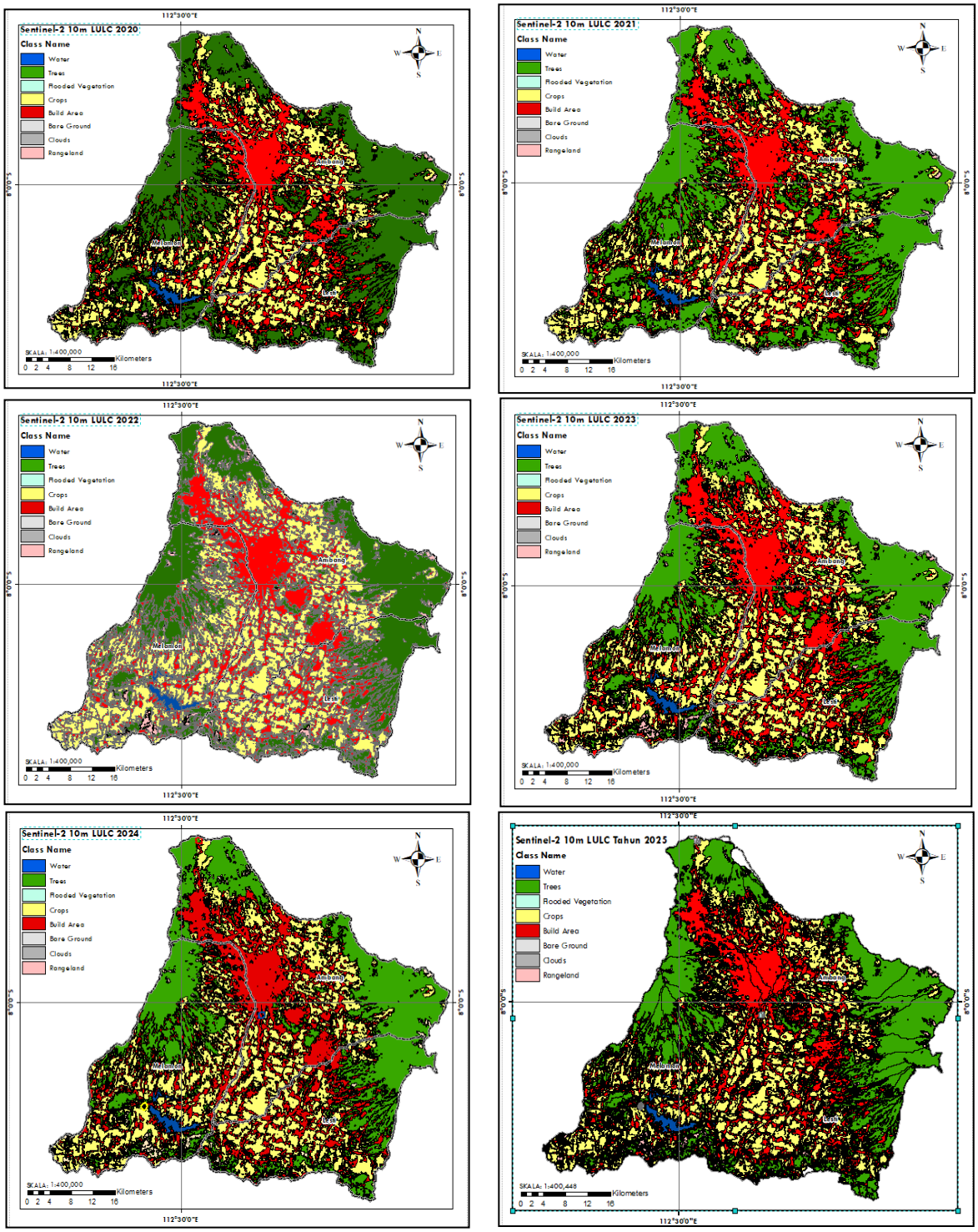

Figure 5. Land cover classification maps of the Upper Brantas watershed for the period 2020-2025

Figure 6. Percentage of land use distribution at three monitoring stations (ST1–ST3) for the period 2020-2025

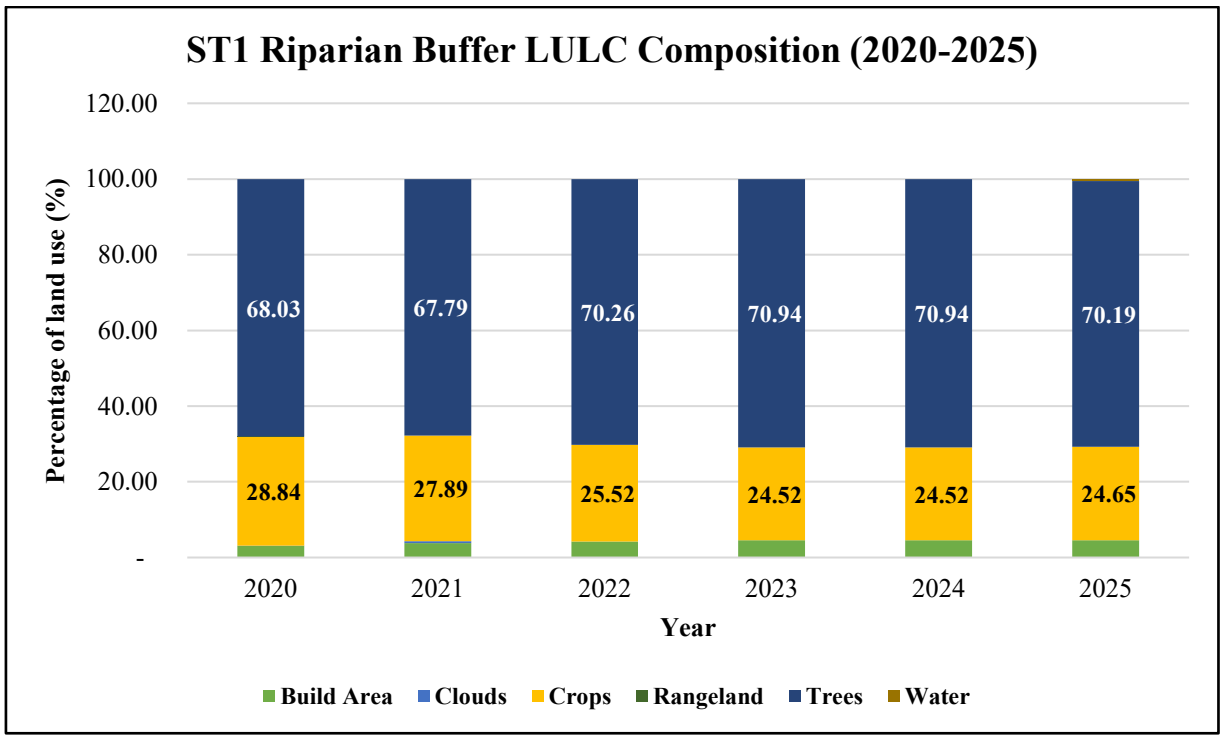

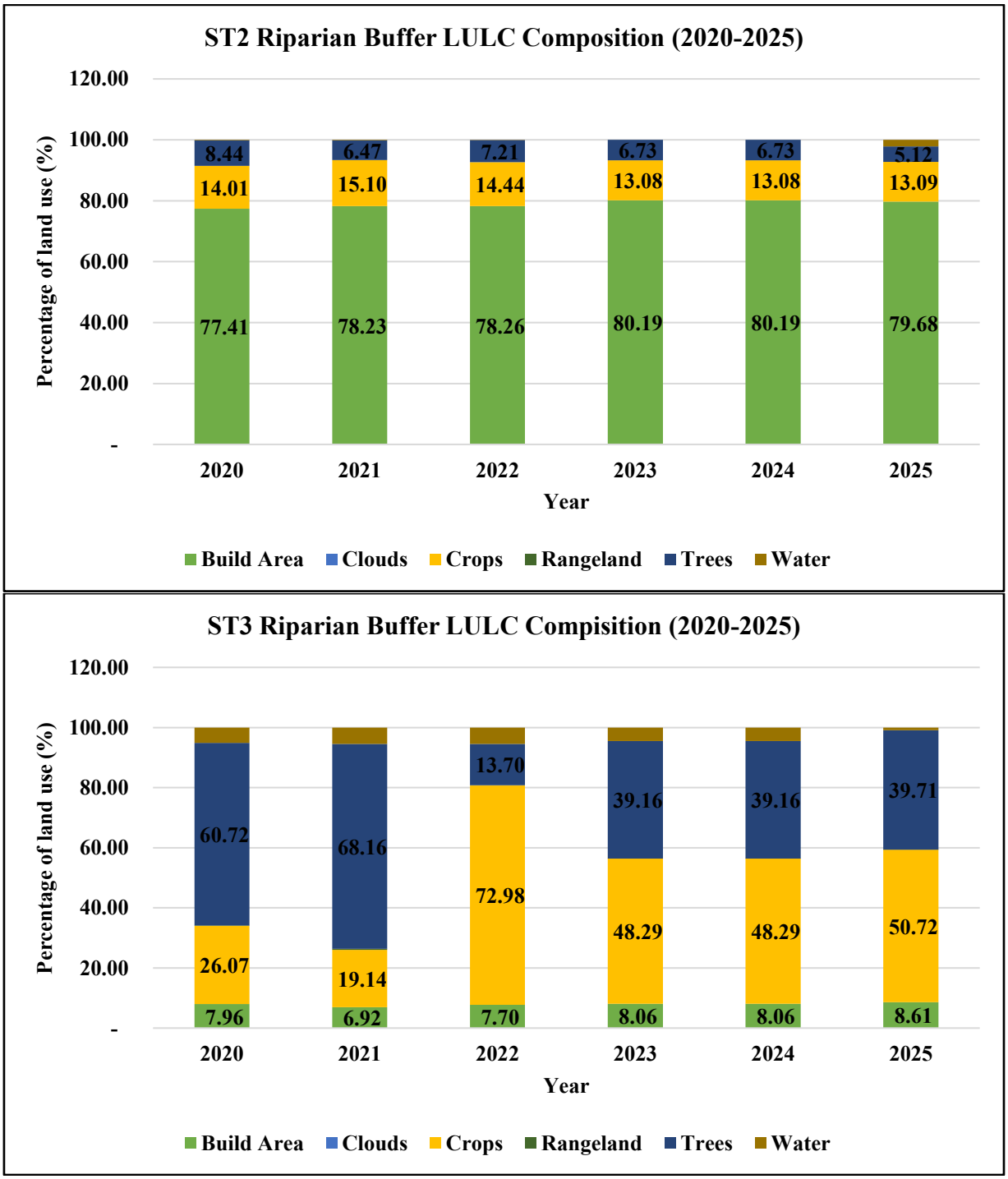

Figure 7. Stacked area plots of built-up, cropland, and forest proportions within the riparian buffer zones of (a) ST1, (b) ST2, and (c) ST3 for the period 2020–2025

The results of the analysis show that during the five-year period, the riparian buffer zones at the three monitoring stations (ST1, ST2, and ST3) underwent changes in land cover. In ST1, built-up areas increased by 1.5% and water areas increased by 0.6%, but there was a 4.2% decrease in agricultural land and a 2.2% decrease in tree cover.

At ST1, the built-up area increased by 1.5%, and the water area increased by 0.6%, but there was a 4.2% decrease in agricultural land and a 2.2% decrease in tree cover. At ST2, a similar pattern of change occurred, with the built-up area increasing by 2.3%. Compared to the other two stations, the dynamics of change at ST3 were greater. The amount of agricultural land increased by 24.7%, but this increase was followed by a 21% decrease in tree cover and a 0.1% decrease in rangeland.

3.5 Principal component analysis

PCA was performed to identify the latent structure between water quality parameters. A KMO value of 0.639 indicates an adequate sample size, while Bartlett's Test is significant (χ^2 = 81.695; $p < 0.001$), indicating a strong correlation between variables, making component extraction feasible. The Total Variance Explained results show that the two main components with eigenvalues > 1 explain 59.58% of the total variance, in accordance with the elbow point pattern on the screen plot, which indicates that the two components are the optimal representation of the data structure. The anti-image

matrix shows that most MSA values are > 0.50, except for DO, which has a low MSA, but this variable is still included in the analysis because it plays an important role in the structure of the second component.

Table 6. Extracted VFs from the 8 parameters of water quality

Parameter	VF1	VF2
TP	0.782	
TSS	0.757	
FC	0.676	
pH	0.656	
DO		-0.799
NO_3	0.503	0.678
COD		0.665
BOD		0.602

The rotated component matrix results (Table 6) show that Component 1 represents variables related to organic pollutant and nutrient loads. This component is characterized by high loading values for TP (0.782), TSS (0.757), Fecal Coliform (0.676), pH (0.656), COD (0.665), BOD (0.602), and Nitrate (0.503).

The relatively high values in the component transformation matrix (0.842 for the diagonal component and 0.540 and 0.842 for the cross values, respectively) indicate that varimax rotation produces stable and orthogonal factor separation, thereby improving the interpretability of the two principal components.

The PC1 and PC2 load diagrams (Figure 8) are presented to improve the readability of the PCA results. These diagrams illustrate the contribution and orientation of each water quality parameter in a two-dimensional PCA space.

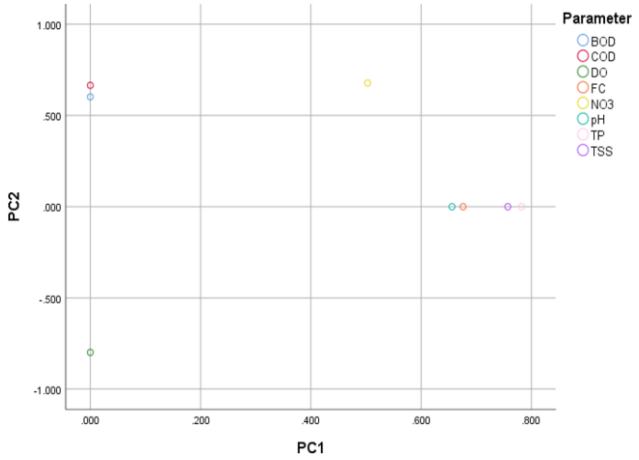

Figure 8. The principal component analysis (PCA) loading plot

3.6 Correlation analysis between the LULC changes and water quality

Multi-temporal analysis was used to assess the relationship between LULC changes and water quality in the Upper Brantas sub-basin. The correlation between annual LULC changes at the Euclidean distance scale at three water quality monitoring stations was calculated and presented in Table 7.

Table 7. Spearman correlation coefficients between the LULC and water quality parameters

	ST1				ST2				ST3			
	Build Area	Crops	Trees	Water	Build Area	Crops	Trees	Water	Build Area	Crops	Trees	Water
pH	0.705	-0.770	0.728	0.564	0.772	-0.679	-0.577	0.525	0.655	0.213	-0.087	-0.339
BOD	-0.247	0.213	-0.239	-0.494	-0.370	0.463	-0.030	-0.278	-0.655	-0.577	0.638	0.000
COD	0.370	-0.395	0.717	0.555	0.926**	-0.741	-0.334	.926**	-0.393	0.213	-0.058	-0.309
TSS	0.953**	-.938**	.862*	0.906*	0.370	0.000	-0.577	0.278	-0.131	0.152	-0.058	-0.185
DO	-0.751	0.708	-0.546	-0.798	-0.093	0.463	-0.030	-0.093	-0.131	0.030	0.058	0.000
NO_3	-0.370	0.213	-0.120	-0.370	.833*	-0.741	-0.213	.926**	0.655	0.820*	-.928**	0.309
TP	-0.073	0.072	0.141	0.237	-0.309	-0.062	0.395	-0.154	0.141	-0.164	0.313	-0.733
FC	0.062	-0.091	-0.239	-0.339	0.432	-0.617	-0.213	0.309	0.531	0.493	-0.485	0.172

ρ = Spearman rank correlation coefficient; ** $p < 0.01$; * $p < 0.05$ (two-tailed).

Further Spearman's correlation analysis conducted at three observation points (ST1, ST2, and ST3) showed a consistent relationship between land use patterns in the watershed (DAS) and water quality parameters. A significant negative relationship between forest cover (trees) and NO_3 was found at observation station ST3 ($\rho = -0.928$, $p = 0.008$).

In addition, the results of the study found a very strong and significant correlation between TSS and built-up area (Build Area; $\rho = 0.953$, $p = 0.003$) and between TSS and water bodies (Water; $\rho = 0.906$, $p = 0.013$) at ST1 and a correlation between COD and built-up area (Build Area, $\rho = 0.926$, $p = 0.008$) at ST2. This indicates that intensive land use activities affect suspended sediment load and organic matter content in water. The correlation between TSS and crops of -0.938 was also observed.

4. DISCUSSION

4.1 Influence of land-use gradients on spatial water-quality patterns

The heterogeneous land use composition within the watershed reflects the spatial pattern of water quality parameters along the Upper Brantas River. This type of land use gradient is known to modify the local microclimate, hydrological pathways, and sources of pollutants, thereby shaping the longitudinal variability of the thermal, physical, and chemical characteristics of river water. In this context, the following discussion analyzes how differences in land cover and human activity between monitoring stations influence the observed spatial contrasts in temperature, suspended solids, and organic pollution indicators.

Figure 2 presents the spatial and seasonal distributions of water temperature, TSS, BOD, and COD across the monitoring stations. The temperature at ST1 consistently remained at the lowest range during both the rainy and dry seasons, with narrow variability indicating the thermal stability of forested areas. The existence of dense riparian vegetation is crucial for sustaining these temperature conditions by providing shade and minimizing surface runoff [32]. Conversely, ST2 and ST3 exhibit significantly elevated temperatures, attributable to the absence of a plant canopy and heightened anthropogenic activities. This condition is consistent with findings that river water temperature is controlled by air temperature, solar radiation intensity, land use, and land cover characteristics [33, 34].

The TSS parameter displayed the most pronounced spatial variation among the observed sites. ST2 exhibited significantly elevated TSS levels, especially during the rainy season, with median values surpassing 100 mg/L—far exceeding the river water quality criteria set forth by Government Regulation No. 22/2021. This increase signifies significant runoff and pronounced erosion in metropolitan regions, particularly during heightened rainfall events. Conversely, ST1 and ST3 exhibited significantly reduced TSS concentrations, affected by upstream plant cover and dryland agriculture techniques that enhance soil erosion resilience. This seasonal trend corresponds with prior research indicating that urban regions exhibit significantly greater runoff and erosion hazards compared to wooded or agricultural areas [35, 36].

ST2 was determined to be the most deteriorated river section across all assessed criteria during both the rainy and dry seasons. The findings indicate that urbanization is the primary factor influencing spatial differences in water quality, whereas seasonal dynamics exacerbate pollution loads, especially for parameters affected by runoff and erosion processes [37].

4.2 Temporal drivers of water-quality degradation in the Upper Brantas watershed

The temporal trends discussed in the previous section show significant interannual and seasonal variability in organic, physical, and microbiological water quality parameters across the Upper Brantas River Basin. These fluctuations indicate that both hydrological conditions and human activities modulate pollutant inputs and processes in water flows over time. To interpret these patterns beyond their statistical expression, the following analysis examines how seasonal dynamics, urban expansion, and land use changes interact to drive the observed temporal evolution of BOD, COD, TSS, nutrients, and fecal contamination.

The organic parameters BOD and COD exhibited a distinct geographical gradient from upstream to downstream. ST1 consistently exhibited the lowest results (< 2 mg/L for BOD and 5–10 mg/L for COD), signifying minor organic pollution loads. In contrast, ST2 exhibited significantly elevated BOD and COD values, especially in the dry season, indicating a buildup of domestic wastewater from densely populated residential areas [38]. Values at ST3 remained mild owing to the synergistic effects of minor household activities and agricultural contributions. This pattern corroborates earlier research indicating that urbanized regions with significant impervious surfaces significantly boost BOD, COD, and TSS levels in river systems [39].

The relationship between parameters can be identified through temporal patterns seen in boxplots. Analysis of temporal trends in chemical parameters (Figure 3) for the period 2020-2025 shows that water quality in the Upper Brantas sub-basin is transitioning towards polluted conditions, as indicated by increases in COD, TSS, and microbiology, even though other indicators such as BOD appear to be improving. From 2022 to 2025, BOD values decreased and were relatively more stable, ranging from 2 to 2.5 mg/L. This decrease indicates an improvement in water quality with lower BOD and meets the required quality standards. BOD values determine how much oxygen is needed to stabilize pollutants in wastewater. Testing these parameters provides an overview of the amount of waste that can be naturally decomposed in water [40].

The pH and DO values tended to be stable in the 2020-2023 period, with a mean ranging from 7-8 mg/L, and their variability decreased dramatically in 2025. DO and BOD are classic indicators of water quality degradation. On the other hand, fluctuations in COD and fecal coliform indicate the presence of major anthropogenic factors contributing to changes in surface water quality [41].

TSS concentrations showed high fluctuations with significant spikes in 2021, 2023, and 2025. The presence of outliers reaching concentrations of 167 mg/L indicates extreme erosion, possibly caused by high rainfall and land conversion in those years. These findings are in line with a study [42], which reported that a number of physicochemical parameters of the samples evaluated for their spatial-temporal variability showed higher concentrations due to massive soil erosion and sedimentation. TSS showed a strong temporal pattern in relation to land use changes, especially in buffer zones that reflect the accumulation of sediment runoff from human activities such as agriculture, settlements, and riverbank erosion [43].

Nitrate and TP concentrations showed an increase, especially in 2024-2025. The highest concentrations in this study were found at point ST2, a densely populated urban area close to the market. Previous studies have shown that high TP and NO_3 concentrations can be caused by various factors, including domestic waste, population density, land use changes, non-point sources, and poor waste management [44, 45]. The combination of increased TP and NO_3 exacerbates the risk of eutrophication.

Fecal coliform values were relatively low in 2020–2023 but spiked dramatically in 2024–2025 (to > 100,000 MPN/100 mL). This sharp increase is a serious indicator of microbiological contamination, which is generally associated with domestic waste. Fecal coliform concentrations show strong spatial–temporal variations, with the highest values occurring in areas with high settlement density and during wet periods, indicating a high contribution from urban runoff and waste input from catchment areas. In this study, the highest fecal coliform concentrations were consistently found at point ST2, a densely populated urban area near the market. This pattern confirms that fecal indicator bacteria are highly sensitive to changes in land use and hydrological conditions [43, 46]. As shown in Figure 4, the increasing frequency of high COD, TSS, and fecal coliform values after 2022 coincides with the expansion of built-up areas and intensified runoff processes in the catchment. The time series evaluation aims to evaluate data sorted based on previous observations while projecting future events.

Observations during the 2020-2025 period show that BOD

concentrations tend to be high in the first two years, namely 2020-2021, and in the last year of observation. BOD concentrations increase during the dry season, indicating that during the dry season, river flow and other water bodies. Reduced dilution causes higher concentrations of organic pollutants [47].

DO concentrations were also found to be lower during the dry season at the ST2 monitoring station in urban areas. These low concentrations were influenced by the high surface water temperature of rivers, which has the ability to retain oxygen. As a result, the available oxygen is reduced. According to the research of Kamarudin et al. [42], which reinforced these findings, Spearman's correlation test shows a weak correlation between DO and COD and DO and BOD during the dry season. This study also found that anthropogenic activities in urban areas have a significant impact on the seasons and the decline in water quality in the Terengganu River, Malaysia.

Surface water quality is shaped by both natural drivers, such as seasonal fluctuations, and anthropogenic inputs originating from settlements, industrial activities, and residential areas [37]. In general, river water quality conditions remain highly sensitive to the combined effects of human disturbances and hydrological variability, underscoring the need for management approaches grounded in ecosystem-based principles.

4.3 Performance and reliability of the ESRI

The confusion-matrix results presented in Table 5 are discussed here to evaluate whether the ESRI CNN-UNet LULC product provides sufficiently reliable classifications for site-specific and buffer-scale analysis in the Upper Brantas River Basin. For the period 2020–2024, the LULC maps derived from the ESRI CNN-UNet product have a reported OA of 85.09%, which is comparable to other global 10 m land-cover products such as WorldCover (83–86%) [48]. The local validation for 2025 yielded an OA of 91% and a Kappa coefficient of 0.873, indicating a high level of agreement between the ESRI classification and the independent reference data. Kappa statistics account for chance agreement and therefore provide a more rigorous measure of classification consistency than OA alone [28, 29]. This confusion matrix is derived from 100 spatially homogeneous reference units and provides a site-specific validation of the ESRI CNN-UNet LULC product for the year 2025. The resulting OA (Local OA = 91%) and Kappa coefficient (Local $\kappa = 0.873$) represent a local consistency check of the ESRI classification within the Upper Brantas sub-basin and should not be interpreted as statistically representative accuracy estimates for the entire watershed or as a replication of the global ESRI validation.

4.4 Performance and reliability of the ESRI CNN-UNet LULC product at the site scale

Land cover changes on the Euclidean scale at three upstream Brantas sub-basin river water quality monitoring stations show significant spatial dynamics during the 2020–2025 period. Forests dominated, with a gradual decline accompanied by a moderate increase in settlement area in the ST1 riparian buffer zone. Meanwhile, a significant increase in settlement area was recorded in the ST2 riparian buffer zone, accompanied by a decline in forest and agricultural land cover. In ST3, agricultural land expanded substantially, replacing most of the forest cover.

The changes that occurred at ST3 indicate the dominance of large-scale land conversion to agricultural use. Overall, the trends at the three stations show an increase in development activity and cultivation land expansion, followed by a significant decline in natural vegetation, especially tree cover.

As illustrated by the stacked area plots in Figure 7, land-cover composition within the Euclidean riparian buffers of ST1, ST2, and ST3 exhibits clear spatially differentiated trajectories over the 2020–2025 period. At ST1, forest remains the dominant class throughout the observation period, although a gradual decline is accompanied by a moderate increase in built-up area within the riparian buffer. In contrast, the ST2 buffer shows a pronounced increase in settlement area and a concurrent reduction in forest and cropland, indicating progressive urban encroachment along the river corridor. The ST3 buffer displays a different trajectory, where cropland expands rapidly and replaces a large fraction of forest cover over time.

These station-specific patterns confirm that riparian-scale land-use transitions are highly heterogeneous and cannot be inferred from watershed-wide averages alone. The strong expansion of cropland at ST3 reflects the dominance of large-scale agricultural conversion, whereas the increasing built-up fraction at ST2 highlights the growing influence of urban development within the river buffer zone. Overall, Figure 7 demonstrates a consistent trend of development and cultivation expansion across the three stations, accompanied by a marked decline in natural vegetation, particularly tree cover, which signifies progressive riparian degradation along the Upper Brantas Rive.

4.5 Interpretation of principal component analysis (PCA) results

The dominance of these parameters indicates that PC1 is a factor that describes anthropogenic pressure originating from domestic activities, agriculture, and surface runoff. Meanwhile, Component 2 is dominated by DO (loading -0.799) and Nitrate (0.678), which shows an inverse relationship between DO and nitrogen nutrient availability. This structure describes the dynamics of deoxygenation and potential eutrophication processes that play a role in water quality variation at the spatial and temporal levels.

Variables related to organic matter, nutrients, and suspended solids (TSS, COD, BOD, TP, FC, pH, and NO_3^-) clustered along the positive PC1 axis, confirming that PC1 represents organic-nutrient pollution factors. In contrast, DO is oriented in the opposite direction to NO_3^- along PC2, indicating an inverse relationship between nutrient enrichment and oxygen availability, which reflects eutrophication and deoxygenation processes in the Upper Brantas River.

Overall, the PCA results identified two dominant factors that drive variations in river water quality: (1) components related to organic pollutant-nutrient loads, and (2) components related to water oxygenation conditions. These two components can be used as a basis for determining water quality management priorities and monitoring parameters that are most sensitive to changes in environmental conditions. Meanwhile, the results of Bayesian correlation analysis reveal a strong pattern of interrelationship between water quality parameters that reflects the dynamics of pollutant loads in river systems. Organic parameters such as COD and BOD showed a consistent positive correlation (mean = 0.49; 95% CI = 0.25 – 0.72), as did the relationship between COD and TSS (mean

= 0.42; 95% CI = 0.12 – 0.66), confirming that an increase in organic load generally occurs in conjunction with high suspended solids. In addition, NO_3 has a high positive correlation with COD (mean = 0.52; 95% CI = 0.30 – 0.74), indicating that the contribution of inorganic nutrients also strengthens oxidative pressure on water bodies. Conversely, DO is negatively correlated with NO_3 (mean = −0.39; 95% CI = -0.64 – -0.12), suggesting that an increase in nitrogen compounds may reduce DO availability through decomposition and eutrophication processes. The positive correlation between TP and FC (mean = 0.57; 95% CI = 0.29 – 0.76) further confirms the influence of phosphate-rich domestic waste on water and sanitation conditions. Overall, these results show that organic pollutants, nutrients, and microbiological contaminants interact significantly and contribute to water quality degradation during the monitoring period.

4.6 Interpretation of LULC–water quality relationships

A previous study by Venter et al. [45] using ESRI Sentinel-2 and Landsat 8 imagery successfully identified the spatial correlation between vegetation indices (NDVI) and water quality parameters. ESRI Sentinel-2 was used to monitor land cover changes related to water quality dynamics, providing adequate temporal information for identifying land use changes that impact water quality.

A significant negative relationship between forest cover (trees) and NO_3 was found at observation station ST3 (ρ = −0.928, p = 0.008), indicating that an increase in the proportion of forest cover is associated with a significant decrease in nitrate concentration in water bodies. This confirms the role of riparian vegetation as a natural nutrient filter. A natural buffer zone up to 50 meters wide along water bodies plays an important role in improving water quality [49].

This indicates that intensive land use activities affect suspended sediment load and organic matter content in water. The correlation between TSS and Crops of -0.938 indicates that agricultural practices in the study area do not increase sediment load, which may reflect conservative land management or the existence of vegetative buffer zones that inhibit sediment transport to rivers**.**

The use of agricultural land and built-up areas has a strong correlation and seasonal dependence on water quality parameters such as TSS, BOD, and COD [14]. These findings are in line with the research by Webb et al. [48], which found a positive correlation between built-up land and TSS parameters in a 50-150 m buffer zone. The results of the study reinforce the evidence that forest cover functions as an effective ecological buffer zone in reducing nutrient runoff into water bodies, as found in the Opak watershed by Harahap et al. [50], which confirmed the role of riparian vegetation in minimizing the transport of pollutants from land runoff. Furthermore, the negative correlation between TSS and agricultural area indicates conservative land management practices that can reduce erosion and sediment load, in line with international literature on the effectiveness of soil conservation and vegetative buffers.

The strong negative correlation between forest cover and Nitrate (NO_3^-) observed at ST3 (ρ = -0.928, p = 0.008) reflects the loss of riparian eco-hydrological functions following deforestation. Forests in riparian zones function as biogeochemical filters that retain and transform nitrogen through plant uptake, soil adsorption, and microbial denitrification. Nitrate-rich surface runoff from agricultural and residential areas will reach rivers more quickly when tree cover is reduced. This is due to the shortening of shallow subsurface flow pathways. According to the research of Chen et al. [36], Zhang et al. [22], and Mânica et al. [23] in tropical and subtropical watersheds, deforestation causes increased nitrate export due to reduced root uptake, decreased soil organic carbon, and disruption of anaerobic microsites necessary for denitrification. This is similar to what has been reported in mixed agricultural-forest watersheds in Southeast Asia, where forest loss in riparian buffer zones significantly increases NO_3^- concentrations in rivers through increased fertilizer leaching and surface runoff [18, 44].

The very strong positive correlations between built-up areas and TSS (ρ up to 0.953) and COD (ρ up to 0.926) observed at ST1 and ST2 indicate the dominant influence of urbanization on sediment and organic pollution loads. Urban surfaces are largely impervious, which accelerates overland flow, reduces infiltration, and mobilizes sediments, hydrocarbons, and organic waste into drainage networks. The expansion of settlements around ST2 has not been matched by the development of rainwater management infrastructure, such as retention ponds or proportional sediment traps. As a result, the rainy season produces intense surface runoff that transports suspended particles and untreated domestic waste directly into rivers. This mechanism is consistent with recent studies of urban watersheds showing that TSS and COD respond strongly to rain-induced surface runoff in areas with high impervious surface cover and limited drainage control [23, 35, 38]. In tropical cities, seasonal rainfall amplifies this effect by washing road dust, organic waste, and sewer leaks into rivers, causing pronounced peaks in TSS and COD during the rainy season [22, 41].

Therefore, the LULC–water quality relationship observed in the Upper Brantas River reflects integrated ecohydrological processes, where forest degradation weakens natural nitrogen retention, while urban expansion, combined with inadequate stormwater management and strong seasonal rainfall, enhances the export of sediments and organic pollutants to surface waters

5. CONCLUSION

Based on the spatio-temporal analysis of water quality and the Euclidean-based riparian buffer assessment conducted at three monitoring stations along the Upper Brantas River from 2020 to 2025, this study synthesizes the key patterns of water-quality variation and their controlling land-use drivers. By integrating descriptive statistics, correlation analysis, and principal component analysis with multi-scale riparian LULC dynamics, the main findings are summarized:

1. Within the Euclidean riparian buffer zones (500 m from the river banks and 1000 m upstream), water quality exhibits a clear spatio-temporal gradient, with ST1 (forested buffer) showing the lowest pollution levels and ST2 (urban buffer) exhibiting the highest TSS, COD, nutrients, and fecal coliform, especially during the rainy season.
2. At the buffer scale, forest cover within the riparian zone is the dominant control on Nitrate (ρ = -0.928 at ST3), whereas built-up land within the same Euclidean buffers is the strongest driver of TSS and COD (ρ up to 0.953 and 0.926 at ST1–ST2).

3. Multivariate analysis (PCA) confirms that organic–nutrient pollution and oxygen–nutrient imbalance within these riparian buffers are primarily driven by urban expansion and forest loss along the Upper Brantas River.

ACKNOWLEDGMENT

The authors would like to thank the Environmental Agency of East Java Province for institutional support related to environmental data and research facilitation. The support and cooperation of colleagues at the agency were invaluable to this study.

REFERENCES

[1] de Mello, K., Valente, R.A., Randhir, T.O., dos Santos, A.C.A., Vettorazzi, C.A. (2018). Effects of land use and land cover on water quality of low-order streams in Southeastern Brazil: Watershed versus riparian zone. Catena, 167: 130-138. https://doi.org/10.1016/j.catena.2018.04.027

[2] Ahmad, W., Iqbal, J., Nasir, M.J., Ahmad, B., Khan, M.T., Khan, S.N., Adnan, S. (2021). Impact of land use/land cover changes on water quality and human health in district Peshawar Pakistan. Scientific Reports, 11(1): 16526. https://doi.org/10.1038/s41598-021-96075-3

[3] Gule, T.T., Lemma, B., Hailu, B.T. (2023). Implications of land use/land cover dynamics on urban water quality: Case of Addis Ababa city, Ethiopia. Heliyon, 9(5): e15665. https://doi.org/10.1016/j.heliyon.2023.e15665

[4] Lintern, A., Webb, J.A., Ryu, D., Liu, S., Bende-Michl, U., Waters, D., Leahy, P., Wilson, P., Western, A.W. (2018). Key factors influencing differences in stream water quality across space. WIREs Water, 5(1): e1260. https://doi.org/10.1002/wat2.1260

[5] Pemerintah Provinsi Jawa Timur. (2024). Information document on the performance of regional environmental management (DIKPLHD) of East Java Province in 2024. Dinas Lingkungan Hidup Provinsi Jawa Timur. https://dlh.jatimprov.go.id/page/laporan-ikplhd-66ece3eb06b11#blog.

[6] Kementerian Lingkungan Hidup dan Kehutanan. (2021). Statistics on water, air, and land cover quality. Direktorat Jenderal Pengendalian Pencemaran dan Kerusakan Lingkungan. https://id.scribd.com/document/671343843/210930123917buku-Statistik-Ppkl-2020-Versi-Cetak.

[7] Mandala, M., Hakim, F.L., Indarto, I., Kurnianto, F.A. (2024). Land use and land cover change in East Java Indonesia from 1972 to 2021: Learning from Landsat. Environmental Research, Engineering and Management, 80(3): 57-69. https://doi.org/10.5755/j01.erem.80.3.35362

[8] Wiwoho, B.S., McIntyre, N., Phinn, S. (2024). Assessing future land-uses under planning scenarios: A case study of the Brantas River Basin, Indonesia. Environmental Challenges, 15: 100873. https://doi.org/10.1016/j.envc.2024.100873

[9] Waskitho, N.T., Wibowo, F.A.C. (2024). Brantas watershed sustainability analysis: Water quality aspects. BIO Web of Conferences, 143: 01013. https://doi.org/10.1051/bioconf/202414301013

[10] Bahri, A.S., Aji, B.P. (2025). Assessment of water quality in the upper Brantas River using macrozoobenthos as bioindicators. International Journal of Design & Nature and Ecodynamics, 20(6): 1419-1426. https://doi.org/10.18280/ijdne.200622

[11] Fulazzaky, M.A. (2009). Water quality evaluation system to assess the Brantas River water. Water Resources Management, 23(14): 3019-3033. https://doi.org/10.1007/s11269-009-9421-6

[12] Roestamy, M., Fulazzaky, M.A. (2022). A review of the water resources management for the Brantas River basin: Challenges in the transition to an integrated water resources management. Environment, Development and Sustainability, 24(10): 11514-11529. https://doi.org/10.1007/s10668-021-01933-9

[13] Umar, Y.P., Susilo, B., Haedriah, A., Setiawan, A., Auliarahma, F. (2025). Land cover quality, pollution, and macrozoobenthos diversity in the Brantas River: Implications for tropical river management. Pakistan Journal of Life & Social Sciences, 23(1): 5655-5665. https://doi.org/10.57239/PJLSS-2025-23.1.00442

[14] Shi, P., Zhang, Y., Li, Z., Li, P., Xu, G. (2017). Influence of land use and land cover patterns on seasonal water quality at multi-spatial scales. Catena, 151: 182-190. https://doi.org/10.1016/j.catena.2016.12.017

[15] Marisi, D.P., Suprihatin, S., Hariyadi, S., Kaswanto, R.L. (2025). The impacts of land use and cover change on water quality of watershed basin. Global Journal of Environmental Science and Management, 11(2): 573-592. https://doi.org/10.22034/gjesm.2025.02.12

[16] Sudjatmiko, H., Bisri, M., Limantara, L.M., Roebijoso, J. (2025). Synthesis on the impact of land cover conversion towards water quantity and quality. Journal of Ecohumanism, 4(3): 70-86. https://doi.org/10.62754/joe.v4i3.6255

[17] Suwardi, Budiastuti, M.T.S., Komariah. (2021). Land use changes impact on water quality in Jeneberang Watershed, South Sulawesi, Indonesia. IOP Conference Series: Earth and Environmental Science, 824(1): 012016. https://doi.org/10.1088/1755-1315/824/1/012016

[18] Guo, Y., Liu, Y., Li, W., Cai, X., Liu, X., Liao, H. (2025). Multi-scale impacts of land use change on river water quality in the Xinxian River, Yangtze River Basin. Water, 17(10): 1541. https://doi.org/10.3390/w17101541

[19] Priyadarshini, R., Hamzah, A., Widjajani, B.W. (2019). Carbon stock estimates due to land cover changes at Sumber Brantas Sub-Watershed, East Java. Caraka Tani: Journal of Sustainable Agriculture, 34(1): 1. https://doi.org/10.20961/carakatani.v34i1.27124

[20] Kurniawati, A., Rayes, L., Suprayogo, D., Sudarto. (2022). Land management and arrangement structure in the Upper Brantas sub-watershed, East Java. Jurnal Geografi: Geografi dan Pengajarannya, 20(1): 41-52. https://doi.org/10.26740/jggp.v20n1.p41-52

[21] Waskitho, N.T., Omenu, M.F., Wibowo, F.A.C. (2024). Sustainability analysis of Upper Brantas Subwatershed. BIO Web of Conferences, 143: 01021. https://doi.org/10.1051/bioconf/202414301021

[22] Zhang, S., Yan, X., Feng, T., Zhang, X., Qiao, R., Ren, Y., Chen, Q. (2025). Unraveling nonlinear impacts of land use change on riverine water quality under future

scenarios. Ecological Indicators, 179: 114258. https://doi.org/10.1016/j.ecolind.2025.114258
[23] Mânica, A.N., Rocha, C., Araújo, L.S., Gomes, R.S., De Lima Isaac, R. (2025). From forest to urban: Assessing the impact of land cover on water quality. Journal of Environmental Management, 386: 125739. https://doi.org/10.1016/j.jenvman.2025.125739
[24] Putra, A.N., Jaenudin, Prasetya, N.R., Sugiarto, M.T., Sudarto, Prayogo, C., et al. (2025). Utilizing remote sensing and random forests to identify optimal land use scenarios and address the increase in landslide susceptibility. Sustainability, 17(9): 4227. https://doi.org/10.3390/su17094227
[25] Warokka, F.Y.M., Suhartini, S., Nugroho, T.W. (2024). The effect of sustainable livelihood assets on the soil and water conservation level adoption in Sumber Brantas Village, Indonesia. Agro Bali Agricultural Journal, 7(3): 878-885. https://doi.org/10.37637/ab.v7i3.1805
[26] Government of Indonesia. (2021). Government Regulation No. 22 of 2021 on Environmental Protection and Management. State Secretariat of the Republic of Indonesia. https://peraturan.go.id/id/pp-no-22-tahun-2021.
[27] Solórzano, J.V., Mas, J.F., Gao, Y., Gallardo-Cruz, J.A. (2021). Land use land cover classification with U-net: Advantages of combining sentinel-1 and sentinel-2 imagery. Remote Sensing, 13(18): 3600. https://doi.org/10.3390/rs13183600
[28] Dash, P., Sanders, S.L., Parajuli, P., Ouyang, Y. (2023). Improving the accuracy of land use and land cover classification of Landsat data in an agricultural watershed. Remote Sensing, 15(16): 4020. https://doi.org/10.3390/rs15164020
[29] Foody, G.M. (2020). Explaining the unsuitability of the kappa coefficient in the assessment and comparison of the accuracy of thematic maps obtained by image classification. Remote Sensing of Environment, 239: 111630. https://doi.org/10.1016/j.rse.2019.111630
[30] Pratama, M.A., Immanuel, Y.D., Marthanty, D.R. (2020). A multivariate and spatiotemporal analysis of water quality in Code River, Indonesia. The Scientific World Journal, 2020(1): 8897029. https://doi.org/10.1155/2020/8897029
[31] Crooks, E.C., Harris, I.M., Patil, S.D. (2021). Influence of land use land cover on river water quality in rural North Wales, UK. JAWRA Journal of the American Water Resources Association, 57(3): 357-373. https://doi.org/10.1111/1752-1688.12904
[32] Li, H., Chen, S., Ruan, X. (2025). Spatial-temporal surface water quality variations in the Huaihe River Basin and quantitation of the influencing factors. Environmental Engineering and Management Journal, 24(8): 1827-1837. https://doi.org/10.30638/eemj.2025.142
[33] Rasul, M.G., Islam, M.S., Yunus, R.B.M., Mokhtar, M.B., Alam, L., Yahaya, F.M. (2017). Spatial and temporal variation of water quality in the Bertam catchment, Cameron Highlands, Malaysia. Water Environment Research, 89(12): 2088-2102. https://doi.org/10.2175/106143017X14839994522740
[34] Yadav, S., Babel, M.S., Shrestha, S., Deb, P. (2019). Land use impact on the water quality of large tropical river: Mun River Basin, Thailand. Environmental Monitoring and Assessment, 191(10): 614. https://doi.org/10.1007/s10661-019-7779-3
[35] Pramaningsih, V., Suprayogi, S., Purnama, I.L.S. (2020). Pollution load capacity analysis of BOD, COD, and TSS in Karang Mumus River, Samarinda. Indonesian Journal of Chemistry, 20(3): 626. https://doi.org/10.22146/ijc.44296
[36] Chen, Y., Yang, Z., Dong, J., Hong, N., Tan, Q. (2024). Understanding phosphorus fractions and influential factors on urban road deposited sediments. Science of the Total Environment, 921: 170624. https://doi.org/10.1016/j.scitotenv.2024.170624
[37] Putro, S.D.S., Wilopo, W. (2022). Assessment of nitrate contamination and its factors in the urban area of Yogyakarta, Indonesia. Journal of Degraded and Mining Lands Management, 9(4): 3643. https://doi.org/10.15243/jdmlm.2022.094.3643
[38] Nguyen, B.T., Vo, L.D., Nguyen, T.X., Quang, N.X. (2020). The interactive effects of natural factor and pollution source on surface water quality in the Lower Mekong River Basin, Southwestern Vietnam. Water Resources, 47(5): 865-876. https://doi.org/10.1134/S0097807820050024
[39] Asfi, M.F., Razak, S.B.A., Zulkifli, M.H., Sharip, Z. (2023). Spatio-temporal factors influencing coliform and Escherichia coli contamination in gross pollutant trap and wetland inlet, Putrajaya, Malaysia. International Journal of Energy and Water Resources, 7(4): 487-498. https://doi.org/10.1007/s42108-022-00233-w
[40] Xu, J., Jin, G., Mo, Y., Tang, H., Li, L. (2020). Assessing anthropogenic impacts on chemical and biochemical oxygen demand in different spatial scales with Bayesian networks. Water, 12(1): 246. https://doi.org/10.3390/w12010246
[41] Naubi, I., Zardari, N.H., Shirazi, S.M., Ibrahim, N.F.B., Baloo, L. (2016). Effectiveness of water quality index for monitoring Malaysian River water quality. Polish Journal of Environmental Studies, 25(1): 1-9. https://doi.org/10.15244/pjoes/60109
[42] Kamarudin, M.K.A., Wahab, N.A., Md Bati, S.N.A., Toriman, M.E., Saudi, A.S.M., Umar, R., Sunardi. (2020). Seasonal variation on dissolved oxygen, biochemical oxygen demand and chemical oxygen demand in Terengganu River Basin, Malaysia. Journal of Environmental Science and Management, 23(2): 1-7. https://doi.org/10.47125/jesam/2020_2/01
[43] Xu, P., Tsendbazar, N.E., Herold, M., de Bruin, S., Koopmans, M., Birch, T., Carter, S., Fritz, S., Lesiv, M., Mazur, E., Pickens, A., Potapov, P., Stolle, F., Tyukavina, A., van de Kerchove, R., Zanaga, D. (2024). Comparative validation of recent 10 m-resolution global land cover maps. Remote Sensing of Environment, 311: 114316. https://doi.org/10.1016/j.rse.2024.114316
[44] Anh, N.T., Nhan, N.T., Schmalz, B., Le Luu, T. (2023). Influences of key factors on river water quality in urban and rural areas: A review. Case Studies in Chemical and Environmental Engineering, 8: 100424. https://doi.org/10.1016/j.cscee.2023.100424
[45] Venter, Z.S., Barton, D.N., Chakraborty, T., Simensen, T., Singh, G. (2022). Global 10 m land use land cover datasets: A comparison of dynamic world, world cover and ESRI land cover. Remote Sensing, 14(16): 4101. https://doi.org/10.3390/rs14164101
[46] Siqueira, T.D.S., Pessoa, L.A., Vieira, L., Cionek, V.D.M., Singh, S.K., Benedito, E., do Couto, E.V.

(2023). Evaluating land use impacts on water quality: Perspectives for watershed management. Sustainable Water Resources Management, 9(6): 192. https://doi.org/10.1007/s40899-023-00968-2

[47] Anima Gyimah, R.A., Karikari, A.Y., Gyamfi, C., Asantewaa-Tannor, P., Anornu, G.K. (2020). Spatial evaluation of land use variability on water quality of the Densu Basin, Ghana. Water Supply, 20(8): 3000-3013. https://doi.org/10.2166/ws.2020.187

[48] Webb, B.W., Hannah, D.M., Moore, R.D., Brown, L.E., Nobilis, F. (2008). Recent advances in stream and river temperature research. Hydrological Processes: An International Journal, 22(7): 902-918. https://doi.org/10.1002/hyp.6994

[49] Laizé, C.L., Bruna Meredith, C., Dunbar, M.J., Hannah, D.M. (2017). Climate and basin drivers of seasonal river water temperature dynamics. Hydrology and Earth System Sciences, 21(6): 3231-3247. https://doi.org/10.5194/hess-21-3231-2017

[50] Harahap, A., Bangun, B., Ilham, C.I., Lumban, D. (2022). Analysis of water quality from bio-physical-chemical factors of the Asahan River North Sumatra. Annals of Forest Research, 65(1): 1513-1528.